Potential effects on atomic motions in liquid alkali metals

S. Ranganathan and K. N. Pathak*
Department of Mathematics and Computer Science, Royal Military College of Canada, Kingston, Ontario, Canada K7K 5L0

Y. P. Varshni
Department of Physics, University of Ottawa, Ottawa, Ontario, Canada K1N 6N5
(Received 28 September 1993)

Molecular dynamics simulations of liquid sodium and cesium have been carried out using the Dagens-Rasolt-Taylor (DRT) interatomic potentials. Results for the static pair correlation function and the velocity autocorrelation function have been obtained and compared with similarly obtained recent data using the Price-Singwi-Tosi (PST) potentials. Both potentials are found to provide excellent agreement with experimental static pair correlation function. Results for the velocity autocorrelation function do not seem to be too different in spite of the fact that the DRT potentials possess no scaling features as exhibited by the PST potentials. However, the mean square displacement of the particles are found to reveal more clearly the effects of differences in potentials.

PACS number(s): 61.20.Ja, 61.25.Mv

I. INTRODUCTION

The structure and dynamics of the liquid state are governed by interatomic potentials, but one of the basic problems in the theoretical study of static and dynamic properties of liquid metals has been the nonavailability of reliable interatomic potentials. However, the situation is much better for liquid alkali metals due to their simplicity in the sense that the Fermi surfaces of conduction electrons in the solid phases are nearly spherical. This enables one to obtain an effective ion-ion interaction within the framework of pseudopotential formalism. For alkali metals, there have been at least two different approaches [1–5] to obtaining an effective ion-ion interaction, which have been found to provide reasonable descriptions of their properties in the solid phases [1,6–12] and to a limited extent in liquid phases [13–15].

The potential obtained by Price, Singwi, and Tosi [1] for the alkali-metal-atom series is based on a simple one parameter Aschcroft pseudopotential model and an electron gas screening function of Singwi, Sjölander, Tosi, and Land [16]. This potential has been used extensively, with success [14,15,17], in the study of static and dynamic properties of liquid alkali metals, particularly liquid rubidium and cesium. An interesting feature of the alkali-metal-atoms potentials of Price, Singwi, and Tosi (PST) as noted by Balucani, Torcini, and Vallauri [15] is their scaling behavior, with scaling determined by σ, the position of the first zero, and ϵ, the well depth, of the potentials. This scaling is somewhat similar to that of Lennard-Jones potentials for inert gases. A recent comprehensive computer simulation study [15] using the PST potentials has indicated that the static pair correlation function $g(r)$, the velocity autocorrelation function $\psi(t)$, and the peak positions of the longitudinal current correlation function exhibit these scaling features and are in close agreement with available experimental data [18,19].

The other potential [2–5] that has been widely used in the solid phase is also based on the pseudopotential theory. In this case the pseudopotential parameters were determined by requiring that the first order perturbation calculation of the charge density induced around an isolated ion in an electron gas should be identical to that generated by a full nonlinear calculation [2,3]. This procedure effectively sums the contributions to the pair potential from all orders of perturbation theory but excludes the effects of many body forces. The resulting potential, which is density dependent, contains no adjustable parameters. We have constructed empirical forms of the potential from the table of data provided by Taylor [20]. These Dagens, Rasolt, and Taylor (DRT) potentials have been extensively used in the calculation of solid state properties and an overall good agreement with experiments have been achieved [6–12]. But so far, DRT potentials have not been used in the study of dynamical correlation functions in the liquid phases of alkali metals.

In this paper we use the DRT potentials to calculate the static pair correlation function, the velocity autocorrelation function (VACF), and the mean square displacement (MSD) of liquid sodium and cesium using the molecular dynamics technique. The frequency spectrum of VACF and its associated memory function have also been obtained. Results are compared with similarity obtained data by Balucani, Torcini, and Vallauri from a PST potential which exhibit scaling features. It is found that DRT potentials do not possess the scaling behavior for the alkali-metal-atom series but both of the potentials provide excellent agreement with experimental values of $g(r)$ [21], and the results for VACF are not very much

*On leave from Department of Physics, Panjab University, Chandigarh 160014, India.

different. The two potentials yield the same value of the self-diffusion coefficient for liquid cesium and are in agreement with the experimental value, while for liquid sodium they differ by about 20%. These differences will obviously be reflected in their respective MSD's.

In Sec. II we describe the properties of DRT potentials for all liquid alkali metals for completeness and compare them with PST potentials. Some details of our molecular dynamics computer simulation are given in Sec. III. Results and a discussion are presented in Sec. IV.

II. INTERATOMIC POTENTIALS

The DRT potentials $u^*=u/\varepsilon$ for all alkali liquid metals are plotted as a function of $r^*=r/\sigma$ in Fig. 1, where ε is the well depth and σ is the position of the first zero of the potential. Here dot-dashed, dashed, dotted, small-dashed and solid curves represent the potentials for Li, Na, K, Rb, and Cs, respectively. The potentials have a hard core, an attractive bowl, and the long range oscillation characteristics of liquids metals. It is clearly seen that these potentials do not have the scaling features exhibited by PST potentials. The well depth parameters ε are plotted in Fig. 2, where crosses and diamonds denote the values for PST and DRT potentials, respectively. As one goes from the light to the heavy alkali-metal-atoms, it is seen that ε decreases from Li and Na then increases for K, Rb, and Cs for the DRT potential, whereas it monotonically decreases from Na to Cs for the PST potential. For a comparative study, we present the (ε,σ) parameters for both potentials in Table I. For the PST potential, it is seen that the number density $n^*=n\sigma^3$ of liquid Na, K, Rb, and Cs at their melting points is almost a constant 0.895 and their melting temperatures $T=\varepsilon T^*/k_B$ correspond to $T^*=0.84$, 0.81, 0.78, and 0.78 for Na, K, Rb, and Cs, respectively. Thus, taking $T^*=0.8$ and $n^*=0.895$ as universal values for the entire alkali-metal-atoms series, one finds that $\varepsilon=567$ K and $\sigma=2.728$ for lithium. These are the values given in the brackets in Table I. It is further noted from the table

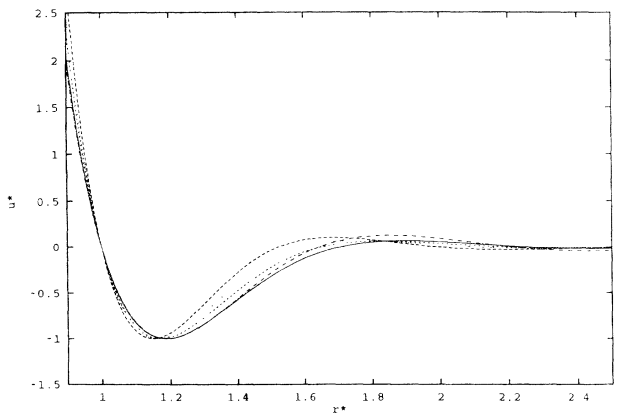

FIG. 1. The DRT interatomic potential $u^*=u/\varepsilon$ plotted as a function of $r^*=r/\sigma$ for liquid alkali metals at densities near their melting points. Li, Na, K, Rb, and Cs potentials are represented by dot-dashed, dashed, dotted, small-dashed, and solid curves, respectively.

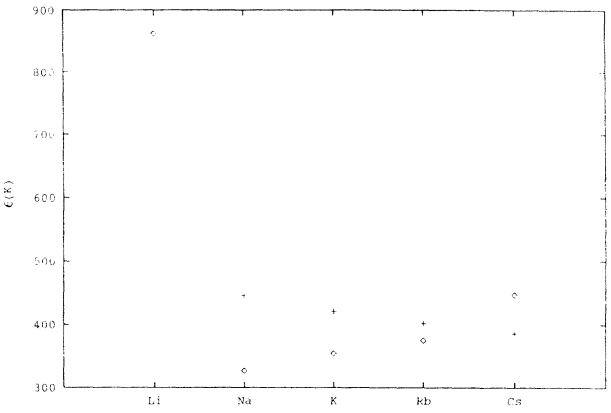

FIG. 2. Comparison of the well depth ε of DRT (diamonds) and PST (crosses) potentials for liquid alkali metals.

that the core radii for the two potentials are close to each other but that their well depth values differ appreciably. A time scale $\tau=(m\sigma^2/\varepsilon)^{1/2}$, often used in computer simulations, for these potentials is also given in the table.

For our computer simulation study, we have chosen liquid Na and liquid Cs only. Potentials for these are plotted in Figs. 3(a) and 3(b), respectively. The corre-

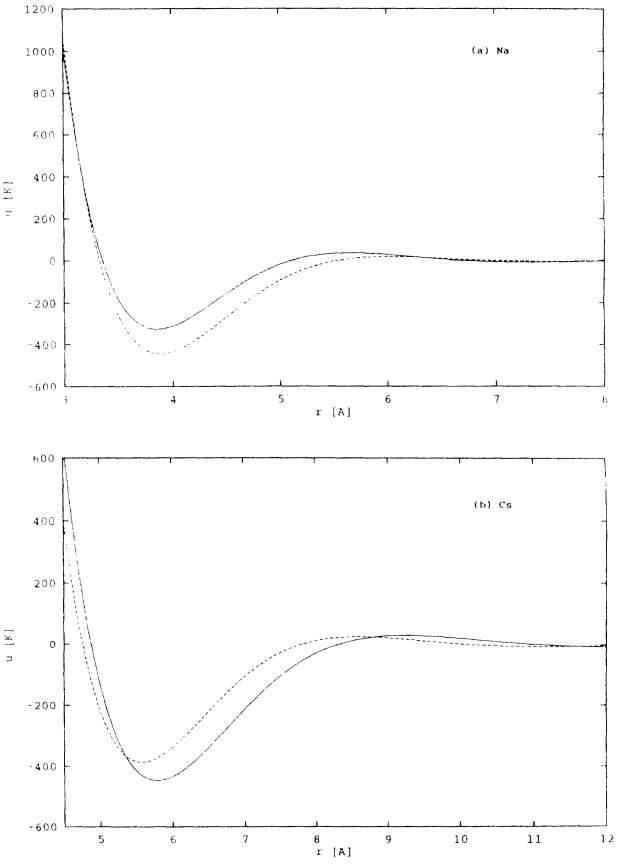

FIG. 3. Comparative plots of DRT and PST potentials are shown by solid and dashed curves, respectively: (a) for Na and (b) for Cs.

TABLE I. Parameters of potentials.

	DRT potential			PST potential		
	σ (Å)	ε (K)	τ (ps)	σ (Å)	ε (K)	τ (ps)
Li	2.642	861.9	0.262	(2.728)	(567)	(0.323)
Na	3.355	327.0	0.979	3.328	445.6	0.832
K	4.162	354.6	1.518	4.115	421.0	1.378
Rb	4.480	375.3	2.345	4.408	402.2	2.229
Cs	4.878	447.1	2.927	4.761	386.5	3.072

sponding PST potentials have also been drawn by a dashed curve. Both potentials for Na are about the same in the core region but differ appreciably in the range $\sigma < r < 6$ Å. The PST potential for liquid sodium is shallower than the DRT potential, and the amplitude of the first long range oscillation of the latter is larger than that of the former. On the other hand, the DRT potential is somewhat shallower than the PST potential for cesium and the long range oscillations are out of phase. Furthermore, these potentials are different in the hard core region although their hard core diameters differ only by about 2%.

III. MOLECULAR DYNAMICS CALCULATIONS

The molecular dynamics (MD) computer simulations were carried out for a system of $N=256$ particles of mass $m=38.41\times10^{-24}$ g for Na and $m=222.11\times10^{-24}$ g for Cs, at their respective melting points and interacting through the DRT potentials $u(r)$ as given in Figs. 3(a) and 3(b), respectively. The particles were confined to a cubic box of length $L=(N/n^*)^{1/3}\sigma$. The lengths of the respective boxes are 6.49σ and 6.38σ for liquid Na and Cs. The dimensionless units of length r^* and time t^* have been used in the calculations. Using periodic boundary conditions, Newton's equations of motion have been solved employing the Verlet algorithm. The time step for integration is $\Delta t^*=0.0046$, which corresponds to a time increment of 0.45×10^{-14} s and 1.35×10^{-14} s for Na and Cs, respectively. The temperature was controlled by scaling the particle velocities every 50 time steps and equilibrium was considered to be achieved if the temperature drift was within about 2 K. The equilibrium temperatures thus obtained were 378 and 308 K for Na and Cs respectively. After establishing an equilibrium configuration, a MD run has been carried out for 8000 time steps. The position and the velocity vectors $\mathbf{r}(t),\mathbf{v}(t)$ are stored for evaluation of correlation functions.

IV. RESULTS AND DISCUSSION

The molecular dynamics $g(r)$ are calculated from the stored trajectories using the usual procedure and results are plotted in Figs. 4(a) and 4(b) for liquid Na and Cs, respectively, by the solid curve; the $g(r)$ obtained by Balucani, Torcini, and Vallauri using the PST potential are shown by the dashed curve. Experimental results are represented by rectangles. It is seen that the results obtained from both DRT and PST potentials are in excellent agreement with experimental data. Thus, $g(r)$ seems to be insensitive to the differences in potentials. This is due to very little difference in the potentials in the core region $r\sim\sigma$.

We now calculate the velocity autocorrelation function

$$\psi(t)=\langle v_x(0)v_x(t)\rangle/v_0^2 , \quad (1)$$

where $v_0^2=k_BT/m$ is the square of the thermal speed. Results are shown in Figs. 5(a) and 5(b) for liquid Na and Cs, respectively, by solid curves, while those obtained by Balucani, Torcini, and Vallauri using the PST potential are shown by dashed curves. While the general features

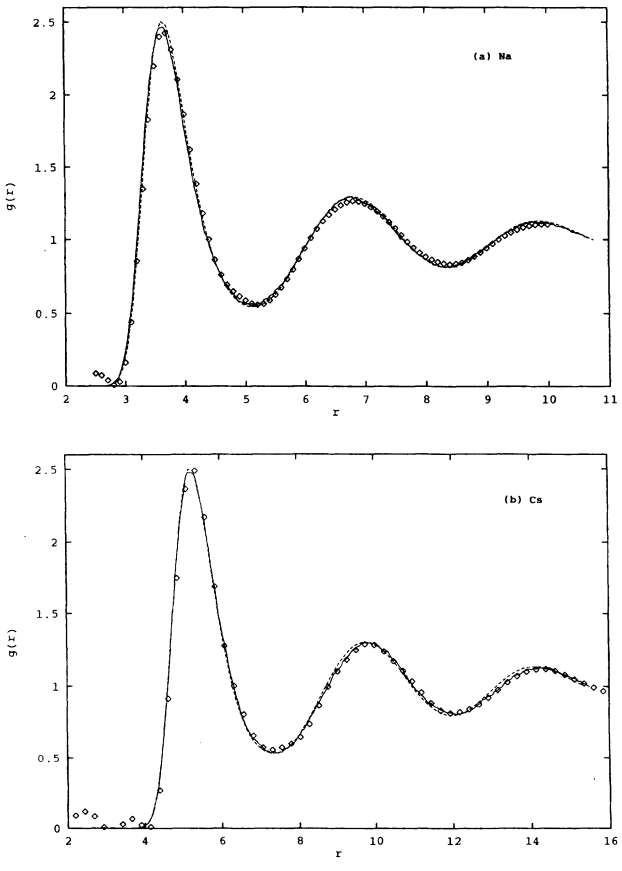

FIG. 4. MD $g(r)$ obtained from DRT (solid curve) and PST (dashed curve) potentials as functions of r: (a) for Na and (b) for Cs. Experimental values are shown by rectangles.

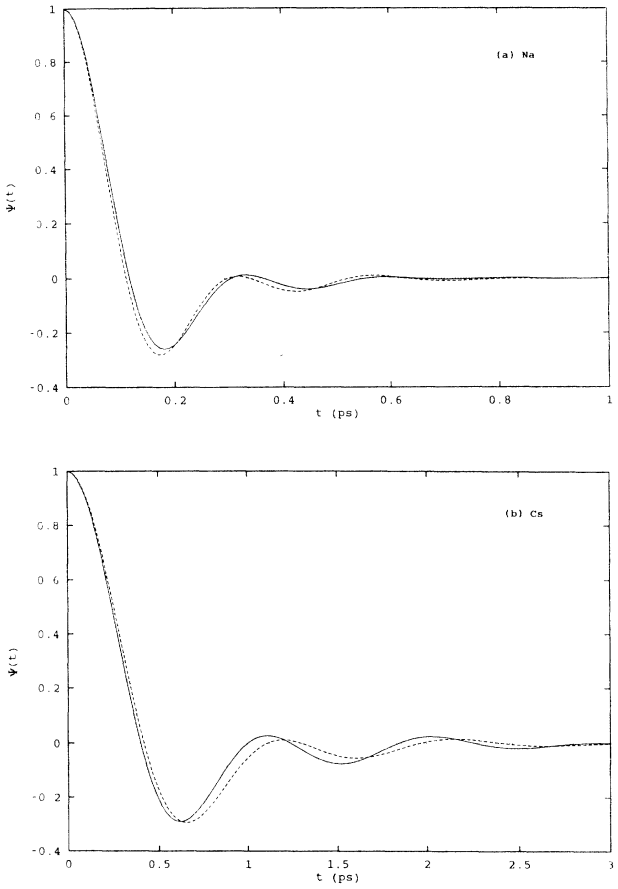

FIG. 5. The velocity autocorrelation function as a function of time for DRT and PST potentials are shown by solid and dashed curves, respectively: (a) for Na and (b) for Cs.

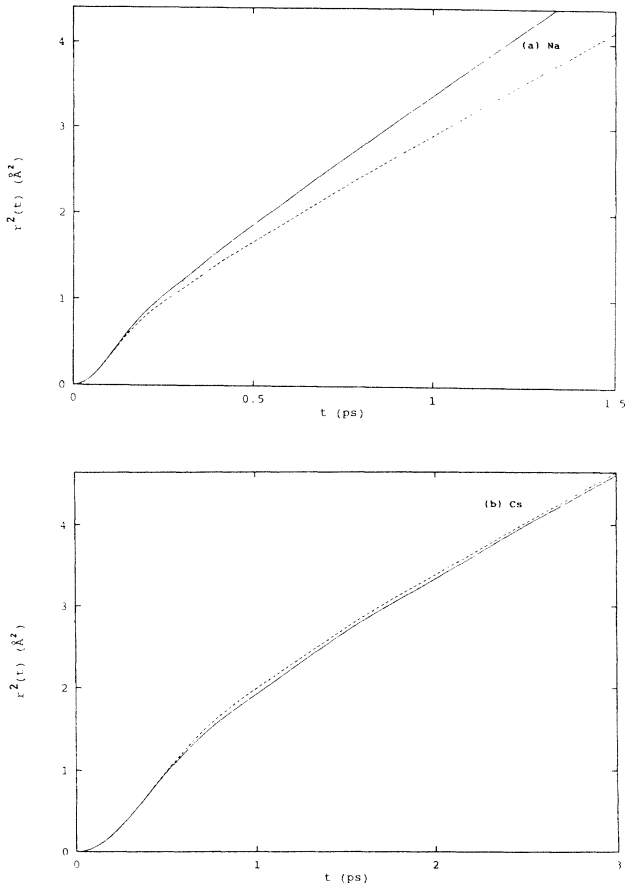

FIG. 6. The mean square displacement as a function of time. The legend is the same as in Fig. 5.

are similar, there are noticeable differences in the time dependence of VACF for the two potentials. The amplitudes of oscillation are somewhat smaller for the PST potentials compared to the DRT potentials and their locations do not match exactly.

Another useful quantity, closely related to the VACF, is the mean square displacement, defined as

$$\langle r^2(t)\rangle = 6v_0^2\tau^2 t^{*2}\int_0^1 dx(1-x)\psi(xt^*)\ , \tag{2}$$

and which in the limit of $t\rightarrow\infty$ yields $6Dt$, where D is the diffusion coefficient. MSD has been calculated directly from the simulation data for DRT potentials and from Eq. (2) using the MD data of $\psi(t)$ for PST potentials. These are compared in Figs. 6(a) and 6(b) for liquid Na and Cs, respectively. It is seen that there are significant differences in the case of Na. Thus it is plausible that potential differences show up more in MSD than in any of the other quantities we have studied thus far.

The diffusion coefficient, which is the area under the $\psi(t)$ curve, is given in Table II. Practically the same diffusion coefficient was obtained from the mean square displacement data. Both potentials gave the same value for the diffusion coefficient of liquid Cs, which is in very good agreement with experimental results [22]. However, the DRT potential for Na predicts a 20% larger diffusion coefficient than that obtained from the PST potential and the experimental value [22]. This is clearly due to the different dynamics generated by the potentials. The identical value of the diffusion coefficient for Cs could be just a coincidence.

The frequency spectrum of the VACF, $f(\omega)$, defined as

$$f(\omega)=\int_0^\infty \psi(t)\cos\omega t\, dt\ , \tag{3}$$

has been plotted in Figs. 7(a) and 7(b) for liquid Na and Cs by solid curve along with the result of the PST potential, shown by a dashed curve. The basic features of both the spectra are similar but there are again visible differences due to potentials. In the spectrum obtained from the PST potential there is a peak and then a flattening in the spectrum for both liquid Na and Cs, whereas

TABLE II. Self-diffusion coefficients D (in units of 10^{-5} cm^2/s) for liquid Na and Cs. D_{MD} and D_{expt} are molecular dynamics and experimental values.

	D_{MD}		
	DRT	PST	D_{expt}
Na	4.95	4.06	4.06–4.35
Cs	2.11	2.11	2.16

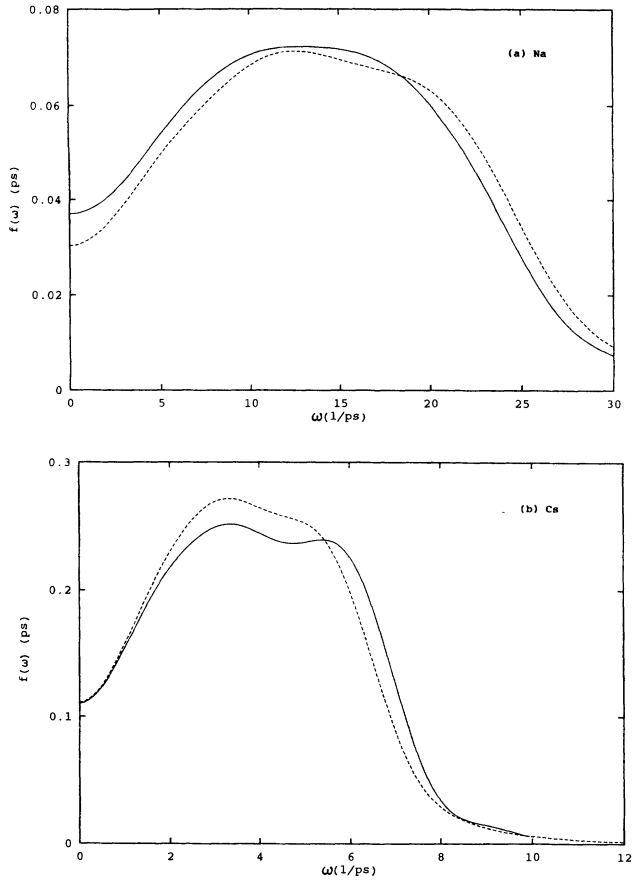

FIG. 7. The frequency spectrum as a function of ω. The legend is the same as in Fig. 5.

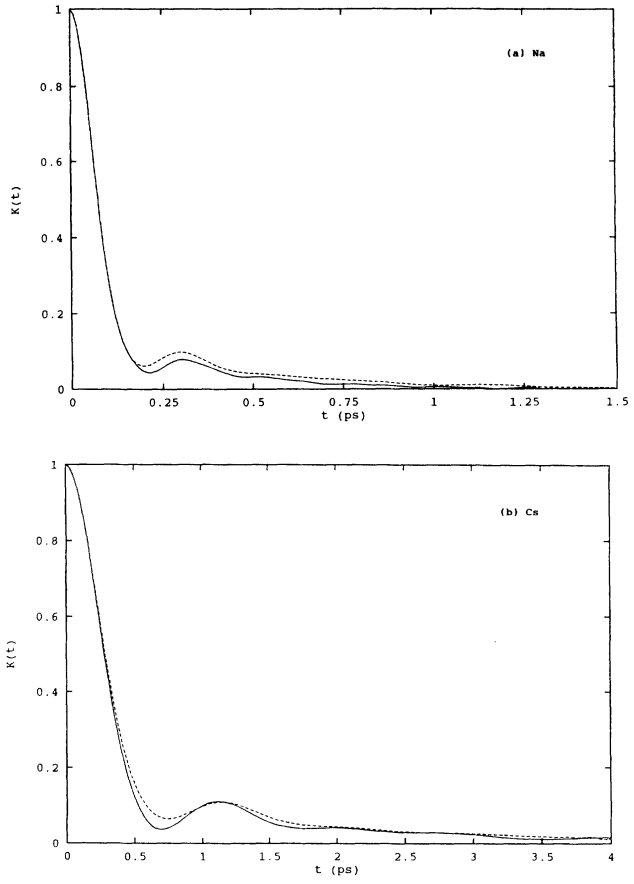

FIG. 8. The memory function, normalized to unity at $t=0$, is plotted as a function of t with the legend the same as in Fig. 5.

there is only a broad peak for Na and a peak and flattening for Cs in the spectra obtained from the DRT potential. The flatness of the spectra does not seem to be an artifact of the calculation. It is probably signaling a different relaxation mechanism [23].

We wish to study the effect of potentials on the memory function associated with VACF and this is extracted from MD data on VACF. The Fourier Laplace transform

$$\tilde{\psi}(z)=i\int_0^\infty e^{izt}\psi(t)dt\ ,\quad z=\omega+i0^+ \tag{4}$$

of VACF has the Mori-Zwanzig representation

$$\tilde{\psi}(z)=-\frac{1}{z+\tilde{K}(z)}\ , \tag{5}$$

where $\tilde{K}(z)$ is the memory function. Therefore, the memory function in the time domain is obtained from

$$K(t)=\frac{2}{\pi}\int_0^\infty \psi''(\omega)\cos\omega t\, d\omega\ , \tag{6}$$

where $\psi'(\omega)$ and $\psi''(\omega)$ are the real and the imaginary parts of $\psi(\omega+i0)$. Results of $K(t)$ are plotted in Figs. 8(a) and 8(b) for Na and Cs, respectively. Here, again, both the potentials reveal the salient features of the liquid memory function, namely, an initial fast decrease followed by a slow relaxation. For liquid Cs the memory function seems to be decaying faster at large times compared to the PST potential. Though there are some quantitative differences between the results of the two potentials, the overall behavior is similar.

In summary, we have presented the molecular dynamics results for $g(r)$ and VACF along with the frequency spectrum, the associated memory function, and the MSD for liquid Na and Cs using DRT potentials. These are compared with similarly obtained data using PST potentials and available experiment results. It is found that $g(r)$ agrees very well with the experimental values as well as with the result from the PST potential. The values of the self-diffusion coefficients for liquid Cs are identical for both potentials, but those for Na differ by about 20%. The overall behavior of VACF is similar. Differences are not appreciable in spite of the fact that DRT potentials possess no scaling features such as those as exhibited by PST potentials. However, it is found that the mean square displacements obtained from the two potentials differ appreciably for liquid sodium, which may indicate that this quantity reveals the effect of potentials more clearly than VACF and $g(r)$. Though it seems that the PST potential provides a value of the self-diffusion coefficient closer to experiment even for liquid Na, we believe that more computer simulation work on dynamical

correlation functions, particularly for liquid Li, is required to sort out potential dependent effects.

ACKNOWLEDGMENTS

We are grateful to Dr. A. Torcini for providing us with computer simulation data for PST potentials. One of us (K.N.P.) acknowledges the partial support of the University Grants Commission, New Delhi, through a research grant. S. R. wishes to acknowledge the support and hospitality of the Department of Theoretical Physics, Australian National University, Canberra, Australia, where part of this work was carried out. This work is supported in part by a grant (ARP-FUHEM) from the Department of National Defence, Canada.

[1] D. L. Price, K. S. Singwi, and M. P. Tosi, Phys. Rev. B **2**, 2983 (1970).
[2] M. Rasolt and R. Taylor, Phys. Rev. B **11**, 2717 (1975).
[3] L. Dagens, M. Rasolt, and R. Taylor, Phys. Rev. B **11**, 2726 (1975).
[4] S. S. Cohen, M. L. Klein, M. S. Duesberry, and R. Taylor, J. Phys. F **6**, L27 (1976).
[5] R. Taylor and A. MacDonald, J. Phys. F **10**, 2387 (1980).
[6] S. S. Cohen and M. L. Klein, Phys. Rev. B **12**, 2984 (1975).
[7] R. Taylor and H. R. Clyde, J. Phys. F **6**, 1915 (1976).
[8] S. S. Cohen, M. L. Klein, M. S. Duesberry, and R. Taylor, J. Phys. F **6**, 337 (1976).
[9] C. R. Leavens, J. Phys. F **7**, 163 (1977).
[10] S. H. Taole, H. R. Clyde, and R. Taylor, Phys. Rev. B **18**, 2643 (1978).
[11] C. R. Leavens and R. Taylor, J. Phys. F **9**, 1969 (1978).
[12] R. Taylor and A. H. MacDonald, J. Phys. F **10**, 2387 (1980).
[13] R. Taylor and A. H. MacDonald, Phys. Rev. Lett. **57**, 1639 (1986).
[14] A. Rahman, Phys. Rev. A **9**, 1667 (1974).
[15] V. Balucani, A. Torcini, and R. Vallauri, Phys. Rev. A **46**, 2159 (1992).
[16] K. S. Singwi, A. Sjölander, M. P. Tosi, and R. H. Land, Phys. Rev. B **1**, 1044 (1970).
[17] A. Torcini (private communication).
[18] J. R. D. Copley and J. M. Rowe, Phys. Rev. A **9**, 1656 (1972).
[19] T. Bodenstainer, P. Morkel, J. Galser, and B. Dorner, Phys. Rev. A **45**, 5709 (1992).
[20] R. Taylor (private communication).
[21] Y. Wasada, *The Structure of Non-Crystalline Materials: Liquids and Amorphous Solids* (McGraw-Hill, New York, 1980).
[22] M. Gerl and A. Brason, in *Handbook of Thermodynamic and Transport Properties of Alkali Metals,* edited by R. W. Ohse (Blackwell Scientific, Oxford, 1985).
[23] W. Gotze and L. Sjogren, Rep. Prog. Phys. **55**, 241 (1992).